Materials Today: Proceedings xxx (xxxx) xxx

Contents lists available at ScienceDirect

Materials Today: Proceedings

journal homepage: www.elsevier.com/locate/matpr

Monitoring of type IV composite pressure vessels with multilayer fully integrated optical fiber based distributed strain sensing

Dorit Munzke [a], Eric Duffner [a], René Eisermann [a,1], Marcus Schukar [a,*], André Schoppa [a], Mariusz Szczepaniak [a], Jörg Strohhäcker [b], Georg Mair [a]

[a] Federal Institute for Materials Research and Testing, Unter den Eichen 87, 12205 Berlin, Germany
[b] Hexagon Purus GmbH, Otto-Hahn-Str. 5, 34123 Kassel, Germany

ARTICLE INFO

Article history:
Received 28 September 2019
Received in revised form 23 February 2020
Accepted 25 February 2020
Available online xxxx

Keywords:
Hybrid composite pressure vessel
Distributed fiber optic sensing
Acoustic emission analysis
Structural health monitoring

ABSTRACT

We present the results of distributed fiber optic strain sensing for condition monitoring of a hybrid type IV composite fully wrapped pressure vessel using multilayer integrated optical fibers. Distributed strain sensing was performed for a total number of 252,000 load cycles until burst of the vessel. During this ageing test material fatigue could be monitored and spatially localized. Critical material changes were detected 17,000 cycles before material failure. Results have been validated by acoustic emission analysis.

1. Introduction

Hydrogen and compressed natural gas (CNG) experience an increased demand as an alternative to traditional energy sources [1,2]. Different possibilities exist for the storage of alternative fuels, whereby high-pressure vessels are becoming more and more popular as gas storage devices in automobiles with pressures up to 700 bar [3]. Modern hybrid composite overwrapped pressure vessels (COPV) consist of a polymer liner fully wrapped with carbon fiber reinforced polymer (CFRP) and glass fiber reinforced polymer (GFRP). The precise knowledge of the vessel condition to guarantee safe usage during lifetime is mandatory. This requires the development of a structural health monitoring system that permits continuous non-destructive evaluation of the filament wound composite pressure vessel on-site, while the tank is still installed in the vehicle. This could be realized during periodic inspection and testing of the COPV and would consequently be favorable for two aspects: control of the periodic inspection and testing itself [4] and usage of gases instead of a corrosive medium.

Detecting damage-induced strains [5] by fiber optic sensors might be an opportunity to monitor material degradation. Swept wavelength interferometry (SWI) based distributed strain sensing (DSS) offers high spatial resolution and can determine truly distributed strain profiles along the entire length of the integrated sensor fiber [6]. SWI based DSS has been used for structural health monitoring of the cylindrical part of a type III COPV with an aluminum liner [7,8] and recently of a type IV COPV during impact test [9].

The capability of acoustic emission (AE) analysis to detect impact defects in COPV followed by subsequent hydraulic pressurization has been subject of investigation within different studies [10,11]. The present study focusses on the failure prediction of an undamaged COPV with acoustic emission testing (AT) during internal pressure lifetime testing. This offers the opportunity for safe usage of the COPV until the end of lifetime without the risk of a catastrophic failure.

The paper deals with the condition monitoring of a type IV COPV with multilayer fully integrated optical fiber based distributed strain sensing covering the entire pressure vessel body including domes, CFRP and GFRP layers. A detailed description of the manufacturing of the pressure vessel is given as well as practical aspects while embedding the sensor fibers. Load cycles test were performed until burst and DSS measurements were accompanied by acoustic emission analysis. This paper stands in context of the research project COD-AGE at the Federal Institute for Materials Research and Testing (BAM), which studied the aging behavior of COPV.

* Corresponding author.
E-mail address: marcus.schukar@bam.de (M. Schukar).
[1] *with BAM until 30.09.2018.*

https://doi.org/10.1016/j.matpr.2020.02.872
2214-7853/

2. Materials and methods

2.1. Manufacturing of the pressure vessel

The composite pressure vessel was fabricated in the manufacturing facility of our industrial collaboration partner Hexagon Purus GmbH. The design of the hybrid type IV COPV was adapted according to state-of-the-art COPV used in automobiles for the storage of CNG at pressures up to 200 bar (test pressure of 300 bar). A schematic drawing of the COPV is shown in Fig. 1.

The composite layers were wrapped by filament winding around a polymer liner (PA 6). The angles of the hoop and helical windings with integrated optical fiber sensors are given in Table 1.

2.2. Installation of the sensor fibers

A polyimide coated 80 μm single-mode optical fiber (SM1500 (4.2/80)P by Fibercore) was embedded and used as the sensor fiber. The diameters of the core, cladding and coating were 4.2 μm, 80.0 μm and 97.0 μm, respectively. This fiber shows a reduced optical bend loss caused by a high germanium-doping and increased numerical aperture. Additionally, the high germanium-doping results in a higher backscatter amplitude.

Four optical fibers were integrated in definite composite layers instantaneously during the wrapping process except for the outermost optical fiber which was wrapped around the COPV before the last hoop winding of GFRP. A surface mounted sensor fiber without any further protection might have been damaged by external impacts. As the optical fibers are directly embedded in the composite layers, the pitch angles of the sensor fibers and the reinforcing fibers are almost identical. Moreover, resin pockets and voids surrounding the individual sensor fibers are reduced [12] (Fig. 2(a,b)). Due to the different installation process, resin rich regions and voids are partly present nearby the outer optical fiber (Fig. 2(c, d)). All relevant information regarding the sensor fibers are summarized in Table 1.

The handling of optical fibers is always challenging, especially regarding the ingress and egress from the composite overwrap [13]. Due to handling reasons, the sensor fibers ingress and egress were either placed at the connection port or the blind end of the pressure vessel. Given by the fact that distributed strain sensing relies on the backscatter signal only a single fiber port is needed. Therefore, the fiber egress could be used as ingress for DSS monitoring as well which gives in total 8 connection ports for 4 embedded optical fibers. The 80 μm sensor fiber was spliced to a standard 125 μm single-mode optical fiber. This reduces transfer losses to the measurement device even over long distances. The different fiber dimensions induce a negligible splice loss.

2.3. Non-destructive testing methods

The artificial ageing of the COPV has been monitored by distributed strain sensing and acoustic emission analysis. A swept wavelength interferometry based optical backscatter reflectometer (OBR 4600, LUNA Inc.) was applied for DSS. The measurement principle is comprehensibly illustrated and described elsewhere [14–16]. Nonetheless, it is important to note that the backscatter amplitude signal-to-noise-ratio in the spatial domain is significant to ensure a good frequency domain cross-correlation contrast and consequently enough accuracy of strain retrieval. A good correlation between measurement and reference spectrum reduces noise. Therefore, data analysis was performed applying the running reference method described in [17].

The spatial resolution of distributed fiber optic strain sensing using an OBR depends on several measurement and post-processing data parameters. A detailed description of the interaction between gage length and sensor spacing is given in [18]. Outliers are reduced by choosing an appropriate gage length and sensor spacing. Here, we selected a maximum device length range of 70 m. The individual sensing range varied according to the total length of the embedded sensor fiber.

Acoustic emission analysis is used to detect material defects emitting acoustic emission. Predominate fast processes like fiber breakage or matrix cracks can be recorded by acoustic emission.

Table 1
Overview of the optical sensor fibers embedded in the COPV.

composite	angle	position	length
CFRP	89.0°	hoop winding onto liner	42.0 m
CFRP	9.5°	helical winding after 32 layers	7.0 m
GFRP	19.0°	outer helical winding	7.2 m

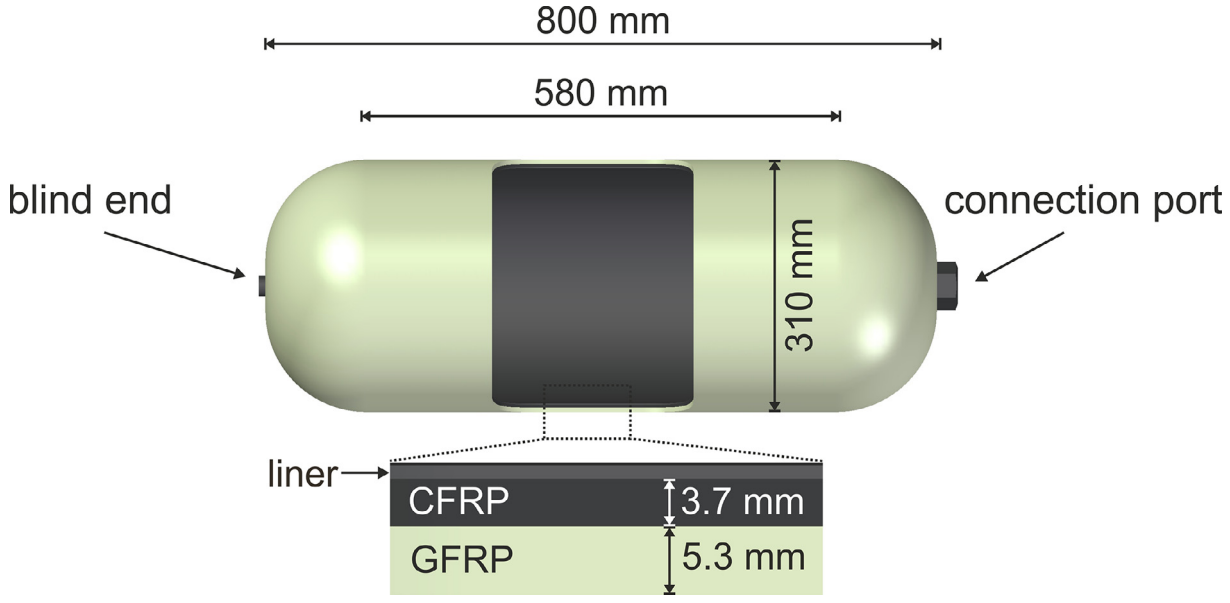

Fig. 1. Schematic drawing of the COPV.

Please cite this article as: D. Munzke, E. Duffner, R. Eisermann et al., Monitoring of type IV composite pressure vessels with multilayer fully integrated optical fiber based distributed strain sensing, Materials Today: Proceedings, https://doi.org/10.1016/j.matpr.2020.02.872

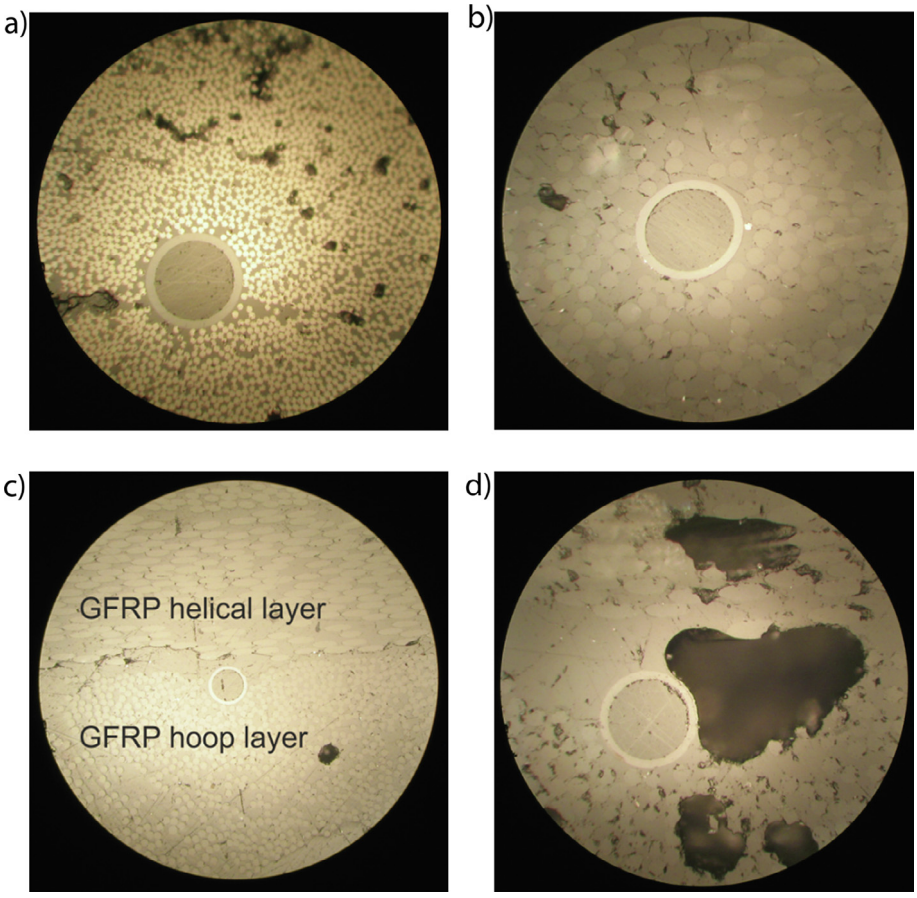

Fig. 2. Post mortem micrograph images of the embedded optical fibers. (a) in CFRP hoop layer; (b) in GFRP helical layer; (c) between GFRP helical and hoop layer; (d) same sensor fiber as left but surrounded by a resin pocket and an air bubble.

The release of elastic energy in such a solid-state body under external load produces an acoustic wave in the material which can be detected by acoustic emission sensors. These mainly piezoelectric sensors transform the acoustic signals into recordable electrical signals. Then, the pre-amplified signals are transmitted to the acoustic emission measurement device. The following acoustic emission analysis allows to evaluate the waveform signals itself (e.g. frequency analysis) or the extracted attributes of these signals (e.g. amplitude). Due to the anisotropic material characteristics of fiber reinforced polymer the propagation of the acoustic emission signal in composites is strongly influenced by the reinforcing fiber direction and the attenuation of the signal. Therefore, an evaluation of the extracted signal features could be in some cases more favorable than the waveform evaluation. Basically, AE can be used for continuous lifetime monitoring of e.g. pressure vessels [19] as well as for short time monitoring of periods with constant pressure (pressure ramps). In this paper, only the AE signals measured during the pressure ramps are evaluated.

2.4. Artificial ageing of COPV

Load cycle tests have been performed in a hydraulic pressure system (PN020, Maximator GmbH). Load cycle tests means a periodically changing internal pressure between a defined lower and upper pressure level for a given time interval and number of load cycles (here: 5000 load cycles with 10 load cycles per minute). A typical pressure-time-diagram is given in Fig. 3(a). Hydraulic load cycle tests have been performed at room temperature and inner pressure loads varying between 20 bar and 260 bar. In order to induce a material failure, first the maximum load cycling pressure was set to 300 bar, which is 1.5 times of the operating pressure, and later on the test temperature was additionally increased to 65 °C. The number of load cycles and the related parameters are given in Table 2. Since the OBR technology only allows for quasi-static measurements, distributed fiber optic sensing was performed during intervals with constant pressure (pressure ramp). The pressure ramps were performed up to a pressure level approximately 10% higher than the above described upper pressure level during load cycling.

The COPV was carefully installed in the hydraulic test chamber (Fig. 3(b)). The patch cables which were spliced to the "ingress part" of 80 μm optical fibers were connected with the output ports of a fiber optical switch (eol 1x4 IR, Leoni). The patch cables which were spliced to the "egress part" of the sensor fibers were not connected. The input port of the fiber optical switch was coupled to the OBR which was controlled by a laptop (OBR v3.12.2, LUNA Inc.). The hydraulic pressure system and the OBR laptop were synchronized using an external control laptop with a self-programmed software application (LabVIEW 2013) and a remote desktop connection. The automatization software was designed to consecutively change the output channels of the switch. This permitted automatic long-term measurements covering thousands of load cycles alternating with pressure ramps for distributed strain sensing measurements.

Five AE sensors were mounted at a center line on the pressure vessel surface starting with sensor 1 (AE S1) in the dome section with the connection port up to AE S5 on the opposite cylinder end close to the dome with blind end (Fig. 3(b)). Wideband AE sensors with a high sensitivity in a frequency range from 100 kHz to 1500 kHz, external pre-amplifiers with a gain of 34 dB, and an

Please cite this article as: D. Munzke, E. Duffner, R. Eisermann et al., Monitoring of type IV composite pressure vessels with multilayer fully integrated optical fiber based distributed strain sensing, Materials Today: Proceedings, https://doi.org/10.1016/j.matpr.2020.02.872

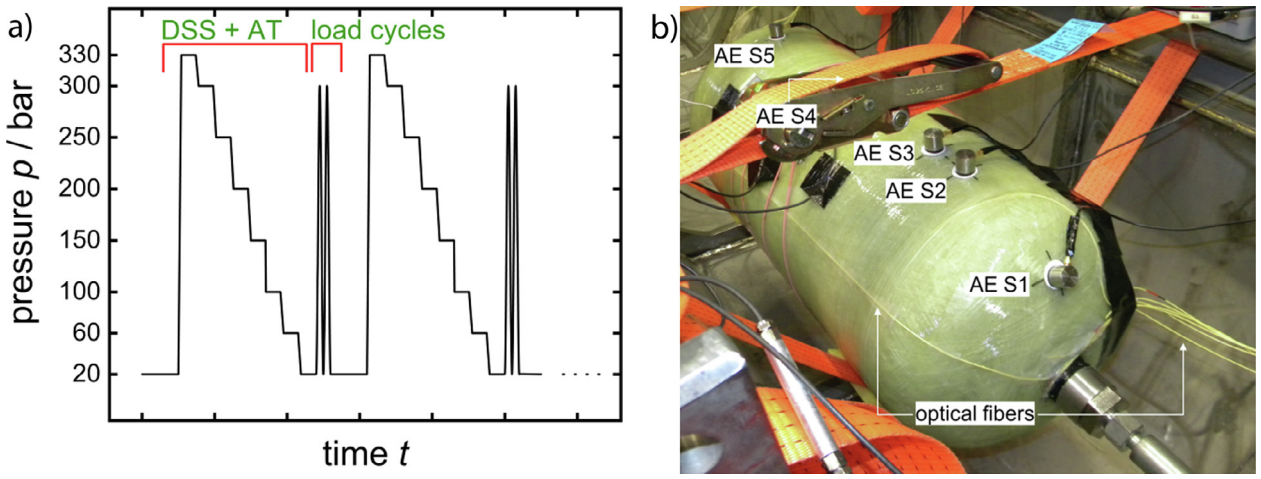

Fig. 3. (a) Pressure-time-diagram used for the last 82,000 load cycle tests before burst. The rates of pressure increase and pressure decrease were set to 50 bar/min and the plateau time to 150 s; (b) COPV installed in the hydraulic internal pressure cycle machine with AE sensors (AE S1 – AE S5) and optical fibers.

Table 2
Load cycles and related parameters.

Number of load cycles	Pressure range	Temperature
170,000	20–260 bar	room temperature
65,000	20–300 bar	room temperature
17,000	20–300 bar	65 °C
total 252,000	pressure vessel burst	

AMSY-6 measurement device (Vallen Systeme GmbH) were applied for the measurements.

3. Results and discussion

3.1. Distributed strain sensing

The strain profile of the sensor fiber integrated in the CFRP hoop layer and measured at 175 bar is displayed in Fig. 4(a). It reflects the manufacturing process of the COPV. First, the strain increases to approximately 6000 μm/m and remains constant until 15 m sensor length. The region between 15 and 20 m belongs to the cylindrical part of the COPV at which the CFRP laminate was attached to the polymer liner which means the beginning of the filament winding. Therefore, the expansion in circumferential direction is reduced due to the accumulation of CFRP layers in this part of the COPV. The inset of Fig. 4(a) zooms in the strain profile and shows the strain distribution over one circumference. The uneven strain profile results from the non-uniform shape of the polymer liner.

Fig. 4(b) shows the backscatter profiles for three serviceable sensor fibers after 235,000 load cycles. Unfortunately, some of the fiber ports have already failed during this part of ageing test. These fiber damages were primarily localized in the connection port or blind end close to the fiber ingress or egress. In total 4 of 8 fiber ports corresponding to 3 of 4 sensor fibers could be utilized until the pressure vessel burst. Both ports of the hoop CFRP sensor fiber failed after 20,000 load cycles, whereas the helical CFRP remained intact untill the vessel burst. As can be expected the local damage of a sensor fiber causes an increased reflection (see sensor fiber ends in Fig. 4(b)). The reflections of these newly formed sensor fiber ends are approximately −50 dB/mm in this averaged resolution (approximately −40 dB/mm in full resolution). Due to the high backscatter amplitude the dynamic range of 70 dB is exceeded, which causes a decreased signal-to-noise-ratio (see noise level amplitudes in Fig. 4(b)) and a lower spatial resolution. Nevertheless, the DSS measurement delivers enough accuracy in strain retrieval for the monitoring application.

The strain profile along the length of the sensor fiber integrated in a GFRP helical layer depending on pressure is displayed in Fig. 5

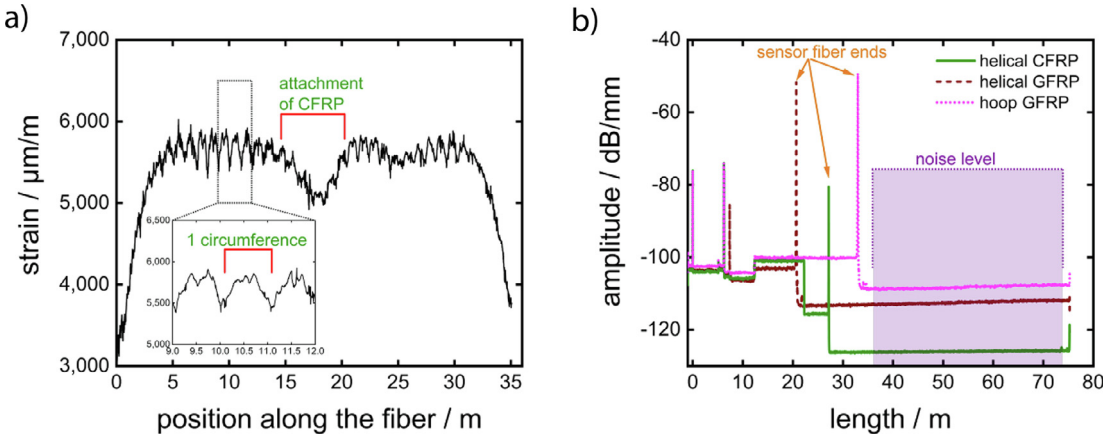

Fig. 4. (a) Initial strain profile along the length of the sensor fiber in the CFRP hoop layer (gage length = 50 mm, sensor spacing = 5 mm) measured at 175 bar; (b) Backscatter profiles of the serviceable sensor fibers after 235,000 load cycles.

Please cite this article as: D. Munzke, E. Duffner, R. Eisermann et al., Monitoring of type IV composite pressure vessels with multilayer fully integrated optical fiber based distributed strain sensing, Materials Today: Proceedings, https://doi.org/10.1016/j.matpr.2020.02.872

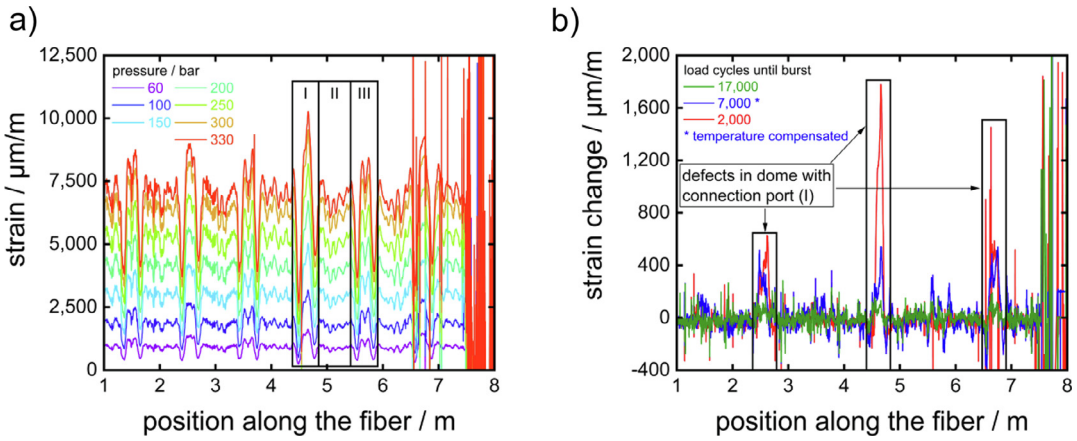

Fig. 5. (a) Strain profile along the length of the sensor fiber integrated in a GFRP helical layer varying with pressure (gage length = 10 mm, sensor spacing = 2 mm). The highlighted areas correspond to dome with the connection port (I), cylindrical section (II) and backside dome with blind end (III); (b) Distributed strain changes along the same sensor fiber measured at 330 bar and varying load cycles until burst.

(a). As expected, the strain increases with increasing pressure. Further the strain profile along the fiber shows a characteristic fingerprint related to the physical position along the vessel. It should be noted that the position of the sensor fiber in relation to the absolute position along the vessel changes slightly with every single wrap. The strain evolution is significant in the dome with the connection port (I) in contrast to the cylindrical section of the pressure vessel (II) and slightly higher compared to the backside dome with blind end (III).

Fig. 5(b) shows the relative strain change along the same sensor fiber for different numbers of load cycles before the vessel burst with respect to a reference strain profile at 65 °C and 330 bar. The three marked sections with increasing strain changes along the length of the sensor fiber correlate with the position of the later material failure. The strain change at 4.6 m is higher compared to the two other peaks. As strain changes are considered to be damage induced, the sensor fiber is closest to the location of material failure. The other two sensor fiber positions are further away of the material damage and, therefore, expect a smaller strain change. These results show the great potential of a fully distributed strain monitoring using integrated sensor fibers compared to local strain measurements. In addition the embedded fiber allows monitoring strain changes in sections of the vessel like close to the connection port which are rather unsuitable for conventional strain detection methods. Typically, high-pressure vessels fail in the cylindrical part of the tank in a so-called safe burst mode [3,20]. Here, the pressure vessel was exposed to extensive cyclic load, which is why material failure in the dome is not unusual. The pressure vessel finally burst after 252,000 load cycles and the connection port was completely ejected from the pressure vessel (unsafe burst mode [3,20]).

The destroyed pressure vessel is shown in Fig. 6. It seems that the connection port lead to local fiber overloads. Typically, the CFRP laminates fail before the GFRP laminates which causes damage progression from the inside out.

The strain profile along the length of the sensor fiber integrated in a GFRP hoop layer for different pressure values is displayed in Fig. 7(a). As expected, the strain increases with increasing pressure, but with slightly higher strain compared to the GFRP helical layer. Moreover, the strain evolution varies and a local strain minimum appears at 1.6 m while increasing the pressure from 60 bar to 330 bar. This can be attributed to the manufacturing process of the COPV with embedded optical fibers. The range between 0 and 2 m belongs to the section of the sensor fiber from ingress to the cylindrical part of the pressure vessel. Changes in the strain profiles are clearly noticeable with increasing pressure which might be due to the presence of reversible opening and closing cracks. Moreover, outliers appear as the pressure is raised to 330 bar, because the sensor fiber end is located within the composite laminate. This leads to variations in the backscatter amplitude of the fiber end (with pressure) and results in a variation of the backscatter noise level, which reduces the accuracy of the correlation-related strain determination.

Fig. 6. Pressure vessel after burst. The tank failed in the dome with connection port, which was completely ejected from the pressure vessel body.

As the outermost sensor fiber is embedded in the GFRP hoop layer covering the cylindrical part of the pressure vessel, strain changes remain almost constant with increasing number of load cycles until burst (Fig. 7(b)). A significant increase in strain change at definite sensor positions as shown in Fig. 5(b) could not be monitored. Instead, an overall increase in random strain change fluctuations could be observed. This might be due to the damaged fiber end located in the GFRP laminate and, therefore, modified correlations.

Please cite this article as: D. Munzke, E. Duffner, R. Eisermann et al., Monitoring of type IV composite pressure vessels with multilayer fully integrated optical fiber based distributed strain sensing, Materials Today: Proceedings, https://doi.org/10.1016/j.matpr.2020.02.872

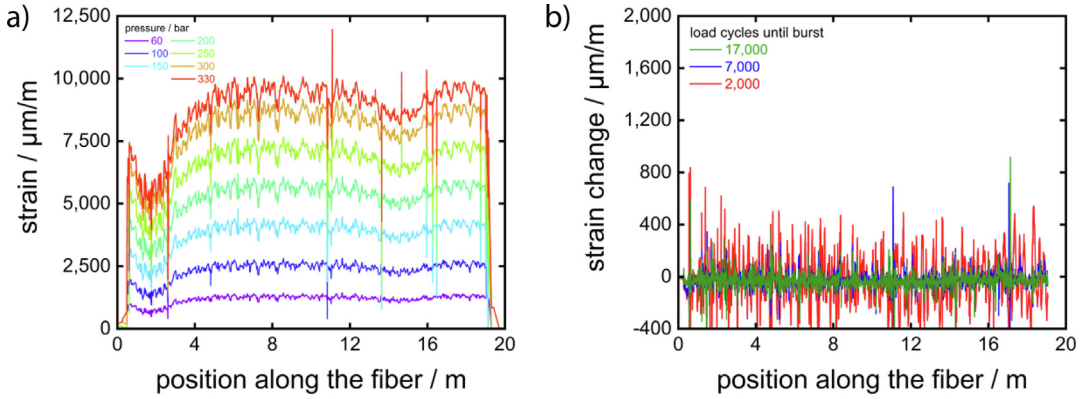

Fig. 7. (a) Strain profile along the length of the sensor fiber integrated in a GFRP hoop layer varying with pressure (gage length = 50 mm, sensor spacing = 5 mm); (b) Distributed strain changes along the same sensor fiber measured at 330 bar and varying load cycles until burst. Data filtered between – 1000 µm/m and 1000 µm/m for clarity reasons.

3.2. Acoustic emission analysis

The data evaluation concerning acoustic emission analysis focus on the pressure ramps to compare the results to those achieved by distributed fiber optic strain sensing. The evaluation of the cumulated energy sum measured for all channels (AE S1 – S5) shows an extreme increase within the last pressure ramp, approximately 2000 cycles before the pressure vessel failure. This is displayed exemplary for channel AE S1 in Fig. 8.

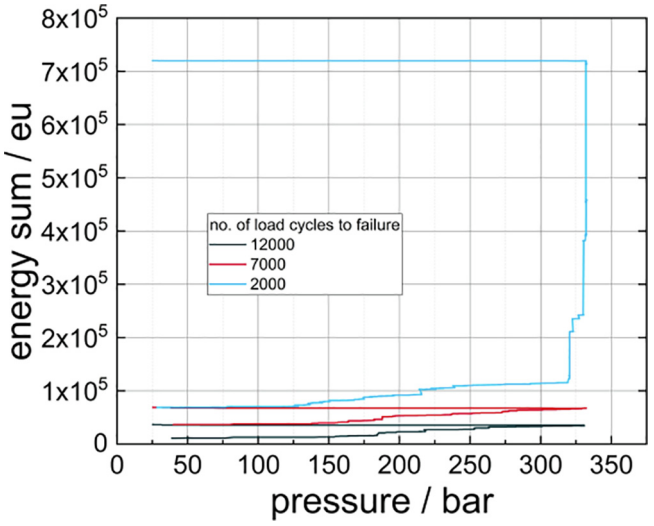

Fig. 8. Cumulated energy sum curve for the last three pressure ramps (approximately 12,000, 7000 and 2,000 load cycles before pressure vessel burst) exemplary to AE S1 located in the dome area with connection port.

For clarity reasons, the cumulated energy sums measured at 7000 and 12,000 cycles before pressure vessel burst are also displayed. Considering the high energy increase during the phase with constant pressure at 330 bar, this must be judged as a critical behavior for composite cylinders and indicates the proceeding damage progress in the composite structure during periods with constant pressure.

The AE energy increase and, therefore, the proceeding damage progress until the end of the pressure vessel lifetime can be detected at each recorded channel (Fig. 9(a)). The channels located close to the final failure region (AE S1 and S2) show the highest total AE energy and, hence, allow a zonal location of the most critical pressure vessel region.

The felicity ratio (*FR*) describes the ratio between the applied load (L_{AE}) and the preceding maximum load (L_{max}) at which significant acoustic emission occurs (1) [19,21].

$$\mathbf{FR} = \frac{\boldsymbol{L_{AE}}}{\boldsymbol{L_{max}}} \tag{1}$$

here, the preceding maximum load equals the maximum pressure during the hydraulic load cycling. The results for the felicity-ratio for all channels (AE S1 – S5) and pressure ramps taken at 65 °C ambient temperature are displayed in Fig. 9(b). Although the

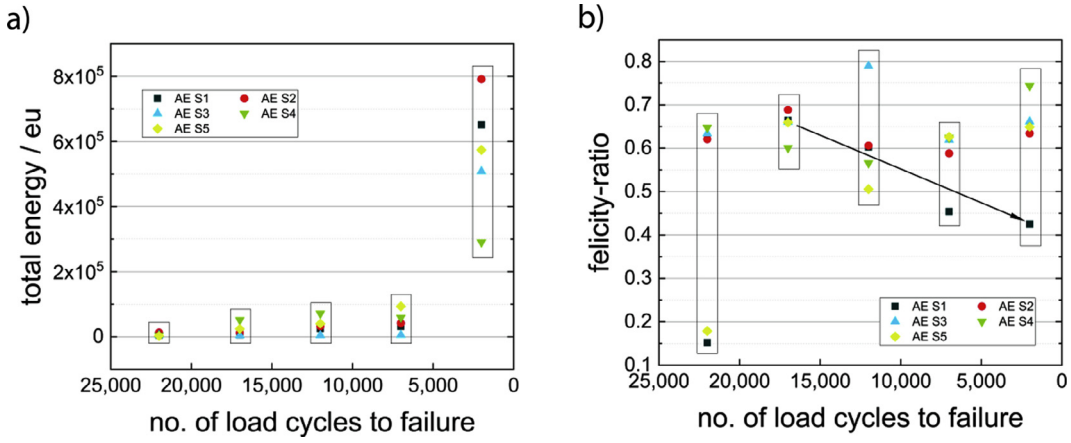

Fig. 9. (a) Total AE energy detected within the pressure ramps, displayed for the number (no) of load cycles to material failure for all channels (AE S1 – S5); (b) Felicity-ratio for all channels (AE S1 – S5) showing a significant decrease of the felicity-ratio for AE S1.

Please cite this article as: D. Munzke, E. Duffner, R. Eisermann et al., Monitoring of type IV composite pressure vessels with multilayer fully integrated optical fiber based distributed strain sensing, Materials Today: Proceedings, https://doi.org/10.1016/j.matpr.2020.02.872

felicity-ratios are relatively low, a continuous decrease for AE S1 from the second to the final period with stepwise pressure variation can be observed. Bearing in mind the significant energy increase, this clearly indicates an upcoming material failure which finally occurred approximately 2000 load cycles after this last pressure ramp.

4. Conclusion

As demonstrated DSS allows for continuous online distributed strain monitoring of type IV COPV with integrated fiber optic sensors. Optical fibers were directly embedded in the composite laminate during the industrial fabrication process including the cylindrical part as well as the domes. Artificial ageing tests with over 250,000 load cycles have been performed until vessel burst with determined elongation of up to 1%. Due to the high mechanical load and high local strain changes, damages of the sensor fibers occurred preferably close to the ingress/egress points at the connection port or the blind end of the pressure vessel. Further investigation on the industrial scale embedding of the fiber could help to avoid or at least reduce fiber defects to improve the reliability of DSS based monitoring of type IV COPV. Nevertheless, three out of four fibers could be used for strain monitoring until the end of the lifetime of the COPV. By measuring damage-induced strain changes material failure could be localized and monitored 17,000 load cycles before burst.

The upcoming cylinder failure could also be clearly detected and confirmed by different acoustic emission evaluation criteria 2000 cycles before pressure vessel burst. The high detection quality, the in-situ measurement and the straightforward and cheap method of applying AE sensors to the vessel surface make AE a good tool for the periodic inspection of type IV COPV.

Declaration of Competing Interest

The authors declare that they have no known competing financial interests or personal relationships that could have appeared to influence the work reported in this paper.

Acknowledgements

We gratefully acknowledge the funding of the research project COD-AGE by the Federal Institute for Materials Research and Testing. We also thank F. Basedau for his support during installation of the sensor fibers, S. Pötschke for his assistance in data analysis and experiments, and M. Bistritz for the preparation of the polishing samples. Special thanks go to Hexagon Purus GmbH for the excellent cooperation and manufacturing of the modified pressure vessels.

References

[1] C. Red, Pressure vessels for alternative fuels, 2014-2023 Available online: https://www.compositesworld.com/articles/pressure-vessels-for-alternative-fuels-2014-2023 (accessed on Apr 1, 2019).
[2] D.J. Durbin, C. Malardier-Jugroot, Review of hydrogen storage techniques for on board vehicle applications, Int. J. Hydrogen Energy 38 (2013) 14595–14617.
[3] J.P. Berro Ramirez, D. Halm, J.-C. Grandidier, S. Villalonga, F. Nony, 700 bar type IV high pressure hydrogen storage vessel burst – Simulation and experimental validation, Int. J. Hydrogen Energy 40 (2015) 13183–13192.
[4] Gas cylinders — Composite construction — Periodic inspection and testing (EN ISO 11623:2015) 2015.
[5] A. Güemes, A. Fernández-López, P.F. Díaz-Maroto, A. Lozano, J. Sierra-Perez, Structural health monitoring in composite structures by fiber-optic sensors, Sensors 18 (2018) 1094.
[6] D.M. Sánchez, M. Gresil, C. Soutis, Distributed internal strain measurement during composite manufacturing using optical fibre sensors, Compos. Sci. Technol. 120 (2015) 49–57.
[7] S.M. Klute, D.R. Metrey, N. Garg, N.A.A. Rahim, B. Va, In-situ structural health monitoring of composite-overwrapped pressure vessels, SAMPE J. 52 (2016) 7–17.
[8] L. Maurin, P. Ferdinand, F. Nony, S. Villalonga, OFDR distributed strain measurements for SHM of hydrostatic stressed structures: an application to high pressure hydrogen storage type IV composite vessels - H2E project, INRIA (2014) 930–937.
[9] E. Saeter, K. Lasn, F. Nony, A.T. Echtermeyer, Embedded optical fibres for monitoring pressurization and impact of filament wound cylinders, Compos. Struct. 210 (2019) 608–617.
[10] F. Dahmene, S. Yaacoubi, S. Bittendiebel, O. Bardoux, P. Blanc-Vannet, M. Barcikowski, M. Panek, N. Alexandre, F. Nony, K. Lasn, et al., Use of acoustic emission for inspection of composite pressure vessels subjected to mechanical impact, in 33rd European Conference on Acoustic Emission Testing (EWGAE 2018) 2018, 11.
[11] P. Blanc-Vannet, Burst pressure reduction of various thermoset composite pressure vessels after impact on the cylindrical part, Compos. Struct. 160 (2017) 706–711.
[12] R. Davidson, S. Roberts, 5.28 - optical fiber sensor compatibility and integration with composite materials. In Comprehensive Composite Materials; Kelly, A., Zweben, C., Eds.; Pergamon: Oxford, 2000; pp. 591–606. ISBN 978-0-08-042993-9.
[13] H.K. Kang, J.W. Park, C.Y. Ryu, C.S. Hong, C.G. Kim, Development of fibre optic ingress/egress methods for smart composite structures, Smart Mater. Struct. 9 (2000) 149–156.
[14] R. Eisermann, F. Basedau, D. Kadoke, P. Gründer, A. Schoppa, C. Lehr, M. Szczepaniak, S. John, M. Schukar, D. Munzke, et al., Distributed strain sensing with sub-centimetre resolution for the characterisation of structural inhomogeneities and material degradation of industrial high-pressure composite cylinders. In Proceedings of the Proceedings of 9th European Workshop on Structural Health Monitoring; Manchester, UK, 2018.
[15] M. Froggatt, J. Moore, High-spatial-resolution distributed strain measurement in optical fiber with Rayleigh scatter, Appl. Opt. 37 (1998) 1735–1740.
[16] S.T. Kreger, D.K. Gifford, M.E. Froggatt, B.J. Soller, M.S. Wolfe, High resolution distributed strain or temperature measurements in single-and multi-mode fiber using swept-wavelength interferometry, in: Proceedings of the Optical Fiber Sensors (2006), paper ThE42; Optical Society of America, 2006, p. ThE42.
[17] S. Heinze, A.T. Echtermeyer, A running reference analysis method to greatly improve optical backscatter reflectometry strain data from the inside of hardening and shrinking materials, Appl. Sci. 8 (2018) 1137.
[18] J.H.L. Grave, M.L. Håheim, A.T. Echtermeyer, Measuring changing strain fields in composites with distributed fiber-optic sensing using the optical backscatter reflectometer, Compos. B Eng. 74 (2015) 138–146.
[19] M.A. Hamstad, A discussion of the basic understanding of the felicity effect in fiber composites, J. Acoust. Emission 5 (1986) 95–102.
[20] D. Leh, P. Saffré, P. Francescato, R. Arrieux, S. Villalonga, A progressive failure analysis of a 700-bar type IV hydrogen composite pressure vessel, Int. J. Hydrogen Energy 40 (2015) 13206–13214.
[21] D.E. Weathers, C. Nichols, J. Waller, R. Saulsberry, Automated determination of felicity ratio for composite overwrapped pressure vessels NASA USRP; 2010.

Please cite this article as: D. Munzke, E. Duffner, R. Eisermann et al., Monitoring of type IV composite pressure vessels with multilayer fully integrated optical fiber based distributed strain sensing, Materials Today: Proceedings, https://doi.org/10.1016/j.matpr.2020.02.872